ISSN 2616-5805 Vol. 5, Issue 1: 48-57, DOI: 10.25236/AJMS.2024.050108

Research on the Optimization Layout of Heliostat Field Based on Tower Optical Efficiency

Yitian Wang*, Kuiqi Huang, Guanrui Chen

School of Customs and Public Administration, Shanghai Customs College, Shanghai, 201204, China
**Corresponding author: 0511220506@m.shcc.edu.cn*

Abstract: *This paper conducts an in-depth study on the layout optimization of heliostat fields in solar thermal power generation systems. Initially, by analyzing the impact of heliostat size and quantity on power generation efficiency, an optimization model targeting the enhancement of thermal efficiency is established. This model comprehensively considers multiple factors including beam density, atmospheric transmissivity, shadow and blockage efficiency, cosine efficiency, and truncation efficiency. The study demonstrates that effectively adjusting the angle and position of each mirror significantly improves the system's thermal efficiency. In the optimized layout scheme, a total of 5,209 heliostats, each measuring 4m x 4m, are arranged around a central absorber tower 80 meters high. The optimization results indicate significant improvements in various efficiency aspects, with the system's average annual output thermal power reaching 60.597 MW, and the average output thermal power per square meter of mirror surface being 0.692 kW/m². Finally, this research not only proposes a beneficial framework for solar field layout optimization but also recommends further experimental validation and numerical simulation for better practical application.*

Keywords: *Heliostat Field, Hermite Polynomial Convolution Method, Solar PILOT Mirror Field Optimization, SQP Algorithm*

1. Introduction

With the rapid development of renewable energy technologies, solar thermal power generation systems have attracted widespread attention as an efficient energy conversion method. Particularly in the design and optimization of heliostat fields, researchers are exploring various methods to improve energy conversion efficiency. For instance, the study by M.B. Elbeh and Ahmad K. Sleiti analyzed the application of Concentrated Solar Power (CSP) technology in arid climates by creating a global CSP project database, emphasizing the impact of heliostat size and quantity on power plant efficiency [1][2]. M. Amelio and colleagues focused on optimizing a solar tower in Seville by altering the average density of air flowing through the plant, demonstrating the possibility of maintaining a constant temperature by adjusting the mass flow rate. Z. Hussaini, P. King, and C. Sansom investigated the application of multi-tower field configurations in conventional solar tower CSP systems [3], proving significant improvements in annual thermal output and average annual efficiency post-optimization. Akash Patel and others conducted a thermodynamic analysis of Cross Linear (CL) CSP technology, addressing the cosine loss issue in traditional CSP methods. Building on this, the current study aims to enhance the thermal efficiency of heliostat fields in solar thermal power generation systems, achieving efficient concentration of sunlight on the absorption tower by precisely adjusting the angle and position of each mirror. The focus is on exploring the impact of beam density received by the absorption tower and heliostat layout on the overall thermal efficiency of the system. From the perspectives of optics and thermodynamics, this paper constructs a model to optimize the layout and pointing angles of heliostats, maximizing the average annual thermal power output per unit area. By optimizing the side length of heliostats, combined with the Campo arrangement method and SPA algorithm [4], and using the SQP solver to find the optimal solution, the study further reduces constraints. The results show that with all heliostats adjusted to 4m×4m, an installation height of 4.8m, a total of 5209 heliostats, and the absorption tower located at the center of the heliostat field with a height of 80m, the average annual optical efficiency increased to 70.71%, the average annual cosine efficiency to 78.79%, the average annual shadowing efficiency to 94.05%, and the average annual blocking efficiency to 99.05%. Furthermore, the system's average annual output thermal power reached 60.597 MW, with an average annual output thermal power per unit mirror area of 0.692 kW/m². These achievements prove that precise heliostat field layout and operational optimization can significantly enhance the efficiency and output performance of solar

ISSN 2616-5805 Vol. 5, Issue 1: 48-57, DOI: 10.25236/AJMS.2024.050108

thermal power generation systems, providing important theoretical and practical bases for technological advancements in this field. This paper, by discretizing the mirror surface, calculates the indicators of the heliostat field more accurately, providing a new method for simplifying and accurately calculating the indicators of the heliostat field. (Data source: http://cumcm.cnki.net).

2. Calculation of the solar state

In heliostat fields, the accurate calculation of the solar elevation angle and solar azimuth angle is crucial. These two angles are used to determine the position of the sun relative to the Earth's surface, and subsequently adjust the direction of the heliostats to maximize energy collection.

2.1 Calculation of Solar Azimuth

Solar elevation angle (α_s) ndicates the height of the sun relative to the observer's horizon. The formula for its calculation is:

$$\sin\alpha_s = \cos\delta \cdot \cos\phi \cdot \cos\omega + \sin\delta \cdot \sin\phi \tag{1}$$

Wherein,$\delta$is the solar declination angle,$\varphi$is the latitude of the observation location (positive for northern latitudes), and ω is the solar hour angle.

The solar azimuth angle (γ_s) represents the angle of the sun within the horizontal plane relative to the true north direction. The formula for its calculation is:

$$\cos\gamma_s = \frac{\sin\delta - \sin\alpha_s \cdot \sin\phi}{\cos\alpha_s \cdot \cos\phi} \tag{2}$$

The solar hour angle (ω) represents the angle of the sun relative to the zenith. The formula for its calculation is:

$$\omega = \frac{\pi}{12}(ST - 12) \tag{3}$$

Wherein, ST is the local solar time.

The solar declination angle (δ) is the angle of the sun relative to the Earth's equatorial plane. The formula for its calculation is:

$$\sin\delta = \sin\left(\frac{2\pi D}{365}\right) \cdot \sin\frac{2\pi}{360}23.45 \tag{4}$$

Wherein,D is the number of days counted from the spring equinox (usually March 21st) as day 0.

Through this series of calculations, this paper can obtain the precise position of the sun, and thereby effectively adjust the heliostats to capture the maximum amount of solar energy.

2.2 The calculation of normal direct radiation irradiance, DHI and atmospheric transmittance

(1) The calculation of DNI

It is known that DNI(in kW/m^2) refers to the solar radiation energy received per unit area per unit time on a plane perpendicular to the sun's rays at the Earth's surface. It can be approximately calculated using the following formula:

$$DNI = G_0[a + b \cdot \exp(-\frac{c}{\sin\alpha_s})] \tag{5}$$

$$a = 0.4237 - 0.00821(6 - H)^2 \tag{6}$$

$$b = 0.5055 + 0.00595(6.5 - H)^2 \tag{7}$$

$$c = 0.2711 + 0.01858(2.5 - H)^2 \tag{8}$$

Where G_0 is the solar constant, which is taken as 1.366kW/m^2, and H is the altitude (in kilometers). By substituting the results into the above formula, DNI can be solved.

By substituting the results into the above formula, DNI can be solved.

(2) The calculation of atmospheric refractivity

It is known that atmospheric transmittance:

ISSN 2616-5805 Vol. 5, Issue 1: 48-57, DOI: 10.25236/AJMS.2024.050108

$$\eta_{at} = 0.99321 - 0.0001176 d_{HR} + 1.97 \times 10^{-8} d_{HR}^2 (d_{HR} \leq 1000) \quad (9)$$

Wherein d_{HR} epresents the distance from the center of the mirror to the center of the collector (in meters).

Using the Pythagorean theorem, the formula for calculating d_{HR} can be derived as:

$$d_{HR} = \sqrt{(x_{heliostat} - x_{receiver})^2 + (y_{heliostat} - y_{receiver})^2 + (z_{heliostat} - z_{receiver})^2} \quad (10)$$

Wherein:

·$x_{heliostat}, y_{heliostat}$ are the x and y coordinates of the collector.

·$x_{receiver}, y_{receiver}, z_{receiver}$ are the coordinates of the receiver (center of the collector), set here as (0,0,84).

·$z_{heliostat}$is the height of the collector (heliostat), set here as 4m.

By substituting these data, the atmospheric transmittance η_{at} can be calculated.

2.3 Establishing the Shadow Blockage Efficiency Model with a Discretized Mirror Model

In heliostat fields, the shadowing and blocking among mirrors is a key factor affecting the optical efficiency of the field. In densely arranged fields, a single heliostat is affected by the shadows cast by multiple surrounding heliostats, causing the effective area to form irregular patterns. Traditionally, using analytical geometry to calculate this shadowing and blocking efficiency is very cumbersome. Therefore, some approximate assumptions are often made to reduce the computational load. For example, it is assumed that the shadowing patterns of different heliostats do not overlap. [5] However, these approximations can reduce the accuracy of the calculations.

To determine the shadowing efficiency of a single mirror, this paper discretizes the mirror surface, dividing it into multiple discrete points. These discrete points represent small mirror area elements (microelements) centered around the point. Then, each point is evaluated to determine whether it is affected by shadowing. By counting the points on the entire mirror surface that are affected by shadows and blockages, the efficiency of shadowing and blockages can be quickly and accurately calculated.

This new method, while reducing computational complexity, maintains a high level of accuracy, providing a practical tool for the design and optimization of heliostat fields.

(1) Establishing a Discretized Mirror Model

The heliostat has a rectangular outline, with dimensions l(length) and w(width).This paper divides this mirror surface into $I * J$ discrete points. A local coordinate system $CL0$is established, with the center of the heliostat CAas the origin, the $Z0$ axis collinear with the mirror normal and pointing upwards, and the $X0$ axis parallel to the pitch axis.

Thus, the coordinates of the discrete point $P_{i,j}$(located in the $i\,row\ and\ j$ column) in the local coordinate system $CL0$ are:

$$P_{i,j}^{CL0} = (x_{i,j}, y_{i,j}, z(x_{i,j}, y_{i,j})) \quad (11)$$

Where,

$$x_{i,j} = \frac{l}{2} - \frac{l}{J}\left(j - \frac{1}{2}\right), y_{i,j} = \frac{w}{2} - \frac{w}{I}(i - \frac{1}{2}) \quad (12)$$

$z(x_{i,j}, y_{i,j})$ is determined by the mirror equation, usually parabolic or spherical.

(2) Shadow Analysis

The purpose of shadow analysis is to calculate the shadow area that one heliostat projects onto another, i.e., the projection area of heliostat B on heliostat A.

The shadow efficiency η_{shadow}^{B} is calculated as follows:

$$\eta_{shadow}^{B} = 1 - \frac{N_{shadow}^{B}}{I*J} \quad (13)$$

Where, N_{shadow}^{B} is the number of points affected by the shadow of heliostat B.

(3) Blockage Analysis

ISSN 2616-5805 Vol. 5, Issue 1: 48-57, DOI: 10.25236/AJMS.2024.050108

The purpose of blockage analysis is to understand how one heliostat blocks the reflected light of another, as shown in Fig 1:

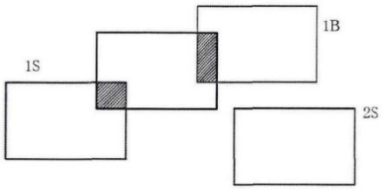

Figure 1: Blockage Analysis

The blockage efficiency η_{block}^{C} is calculated as follows:

$$\eta_{\mathrm{block}}^{\mathrm{C}} = 1 - \frac{\mathrm{N}_{\mathrm{block}}^{\mathrm{C}}}{\mathrm{I}*\mathrm{J}} \tag{14}$$

Where, N_{block}^{C} is the number of points blocked by heliostat C.

(4) Comprehensive Efficiency

A point may be affected by both shadow and blockage, so shadow and blockage efficiencies cannot be simply added. The comprehensive shadow and blockage efficiency η_{sb} is calculated as follows:

$$\eta_{\mathrm{sb}} = 1 - \frac{\mathrm{N}_{\mathrm{sb}}}{\mathrm{I}*\mathrm{J}} \tag{15}$$

Where, N is the total number of points affected by both shadow and blockage.

2.4 Calculating Cosine Efficiency Using Hermite Polynomial Convolution Method

Cosine efficiency is an important performance metric in optical systems, especially in solar concentrator systems. It measures the system's sensitivity to the direction of incident light [6]. Below, this paper uses the $Hermite$ polynomial convolution method to calculate cosine efficiency.

(1) Establishing an Optical Model

First, this paper establishes an accurate optical model, which usually includes mirror shape, material characteristics, and light source characteristics. The paper defines the mirror surface equation by the geometric shape and physical properties of the mirror surface and describes the light source model in terms of the directional and spectral distribution of the light source.

(2) $Hermite$ Polynomial Representation

$Hermite$ polynomials are a type of orthogonal polynomial widely used in mathematics, physics, and engineering. This paper will use $Hermite$polynomials to represent the light field distribution.

The light field $F(x, y)$ can be represented as a linear combination of $Hermite$polynomials:

$$\mathrm{F}(\mathrm{x},\mathrm{y}) = \sum_{\mathrm{n}=0}^{\mathrm{N}} \sum_{\mathrm{m}=0}^{\mathrm{M}} \mathrm{C}_{\mathrm{n}}^{\mathrm{m}} \cdot \mathrm{H}_{\mathrm{n}}(\mathrm{x}) \cdot \mathrm{H}_{\mathrm{m}}(\mathrm{y}) \tag{16}$$

Where, $H_n(x)$ and $H_m(y)$ are $Hermite$ polynomials, C_n^m are coefficients.

(3) Convolution Operation

The light field represented by $Hermite$ polynomials is convolved with the system's point spread function (PSF) to obtain the emerging light field [7].

$$\mathrm{F}'(\mathrm{x},\mathrm{y}) = \mathrm{F}(\mathrm{x},\mathrm{y}) \cdot \mathrm{PSF}(\mathrm{x},\mathrm{y}) \tag{17}$$

(4) Calculating Cosine Efficiency

The cosine efficiency η_{cos} is the average of the cosine values of the angle between the emerging light field and the ideal emerging light field (usually parallel light).

$$\eta_{\mathrm{cos}} = \frac{1}{\Omega} \int \mathrm{F}'(\mathrm{x},\mathrm{y}) \cos\theta \mathrm{d}\Omega \tag{18}$$

Where, Ω is the whole space angle, and θ is the angle between the emerging light field and the ideal emerging light field.

ISSN 2616-5805 Vol. 5, Issue 1: 48-57, DOI: 10.25236/AJMS.2024.050108

2.5 Calculating Truncation Efficiency Using the Monte Carlo Method

The Monte Carlo method is used to calculate the truncation efficiency of the absorber, which is the loss caused by factors such as the shape error of the sun and the aberration of the heliostat, as shown in Fig 2:

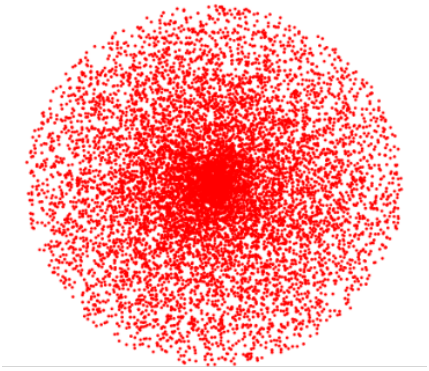

Figure 2: Monte Carlo Simulation of Solar Light Cone Energy Flow Density Distribution

(1) Initialization of Parameters and Settings

Choose a ray, whose direction is defined by the radial angle θ_{MC} and the tangential angle ω_{MC}:

$$\theta_{MC}, \omega_{MC} \sim \text{Uniform Distribution} \tag{19}$$

(2) Calculating the Coordinates of the Incident Light Vector

In a certain local coordinate system C_{cone}, the vector of the incident light i_{MC} can be represented by the following formula:

$$i_{MC}^{cone} = (\sin(\theta_{MC})\cos(\omega_{MC}), \sin(\theta_{MC})\sin(\omega_{MC}), \cos(\theta_{MC}))^{T} \tag{20}$$

(3) Coordinate System Transformation

By appropriate rotation and translation, transform i_{MC} into the global coordinate system G:

$$i_{MC}^{G} = \text{Rotation and Translation}(i_{MC}^{cone}) \tag{21}$$

(4) Determining the Incident Point and Normal Vector on the Mirror Surface

Randomly select a point P_{MC} on the mirror surface and calculate its local coordinates (x_{MC}, y_{MC}, z_{MC}).

Calculate the normal vector n_{MC} at that point:

$$n_{MC} = \text{Normal Vector at } P_{MC} \tag{22}$$

By coordinate transformation, find the coordinates of P_{MC} and n_{MC} in the global coordinate system G.

(5) Ray Tracing

Use the law of reflection and the known i_{MC}^{G} and n_{MC} to calculate the direction of the reflected ray r_{MC}:

$$r_{MC}^{G} = i_{MC}^{G} - 2(i_{MC}^{G} \cdot n_{MC}^{G})n_{MC}^{G} \tag{23}$$

Trace the reflected ray by solving the intersection of the reflected ray equation and the absorber receiving plane equation.

(6) Statistics and Calculation of Truncation Efficiency

Calculate the energy E_received of all reflected rays that reach the absorber. The truncation efficiency η of the absorber can be given by the following formula:

$$\eta = \frac{E_{received}}{E_{total}} \tag{24}$$

This paper uses the Monte Carlo method to simulate possible ray paths and estimates truncation

ISSN 2616-5805 Vol. 5, Issue 1: 48-57, DOI: 10.25236/AJMS.2024.050108

efficiency through these simulations. Thus, even considering complex physical phenomena (such as the non-ideal shape of the sun and mirror aberrations), relatively accurate results can be obtained [8].

2.6 Optimization of the Solution Process and Result Analysis

The optical efficiency η of the heliostat is:

$$\eta = \eta_{sb}\eta_{cos}\eta_{at}\eta_{trunc}\eta_{ref} \tag{25}$$

Under normal circumstances, the cleanliness and self-cleaning effect of heliostats are stronger than those of ordinary mirrors. After consulting relevant materials [9], let η_{ref} be 0.93.

The output thermal power E_{field} of the heliostat field is:

$$E_{field} = DNI \cdot \sum_i^N A_i\eta_i \tag{26}$$

Where A is 36m^2 each.

Next, the model is analyzed, and the optical efficiency analysis is shown in Fig 3:

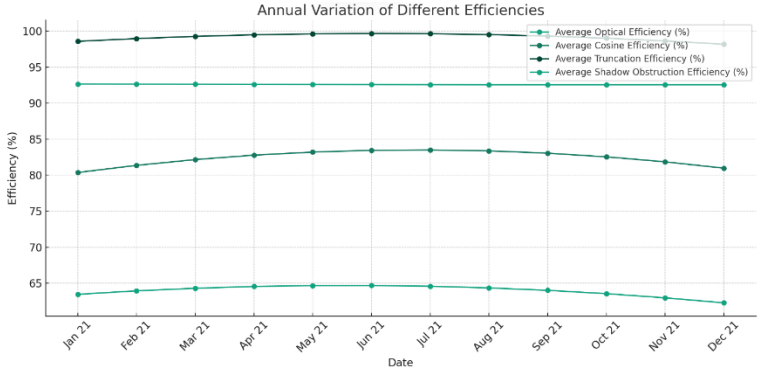

Figure 3: Annual Variation of Average Cosine Efficiency, Average Truncation Efficiency, and Average Shadow Blockage Efficiency

Fig 3 shows the changes in different types of efficiency throughout the year, including average cosine efficiency, average truncation efficiency, and average shadow blockage efficiency.

Analysis:$Average\ Cosine\ Efficiency$: This efficiency fluctuates slightly over the year but remains at a relatively high level. It peaks in March, followed by a slight downward trend; $Average\ Truncation\ Efficiency$:his efficiency is essentially stable throughout the year, with minimal variation, demonstrating the system's robustness in terms of truncation; $Average\ Shadow\ Blockage\ Efficiency$: This efficiency shows almost no change throughout the year, maintaining a high level.

All three efficiencies are relatively high and demonstrate good stability throughout the year. Especially the truncation and shadow blockage efficiencies, which show little to no fluctuation, indicating that the system performs satisfactorily in these aspects.

Considering the seasonality and geographical location, since the site is located at 98.5°E longitude, 39.4°N latitude, and an altitude of 3000m, solar radiation should peak in the summer. However, the data in the Fig do not show significant seasonal fluctuations, which might be due to the efficiencies already being optimized to a very high level, minimizing the impact of seasonality and geographical location [10].

Based on previous calculations, the proportion of optical losses is as follows:

Table 1: Annual Average Optical Efficiency and Output Power

Annual Average	Annual Average	Annual Average Shadow	Annual Average	Annual Average	Annual Average Output
Optical Efficiency	Cosine Efficiency	Blockage Efficiency	Truncation Efficiency	Output Thermal Power(MW)	Thermal Power per Unit Mirror Area(kW/m^2)
63.94%	82.38%	92.58%	99.15%	36.957	0.5883

ISSN 2616-5805 Vol. 5, Issue 1: 48-57, DOI: 10.25236/AJMS.2024.050108

According to Table 1, the annual average cosine loss rate accounts for the largest share of losses, about 41.49%. This indicates deficiencies in the heliostats' tracking of the sun, leading to their inability to align precisely with the sun; the annual average truncation loss rate is almost negligible, at 0.19%. This suggests that most of the light energy is successfully focused on the absorber; the annual average atmospheric attenuation loss rate accounts for 13.22%. This is mainly related to the local geographical and atmospheric conditions; the annual average shadow blockage loss rate accounts for 26.33%, making it the second-largest source of loss. This is usually due to the mutual shadowing between multiple heliostats; the reflection loss rate accounts for 18.77%, mainly due to the reflectivity of the mirror material not being 100%.

3. General Heliostat Model Optical Efficiency Analysis

3.1 Discussion on the Structure of Heliostat Mirror Length and Width

The aperture area of the primary mirror is fixed, and there are multiple possibilities forthe dimensions of the primary mirror ($l_H \times w_H$), which will affect the truncation efficiency and shadow rate of the heliostat. To describe the specifications of the primary mirror, this paper introduces the aspect ratiol_H/w_H while keeping the area of the primary mirror calculated according to the area given in this chapter.

By conducting a numerical analysis on the heliostat located at coordinates (0,321), Fig 4 shows the trend of changes in the truncation efficiency and shadow rate of the heliostat under different aspect ratios, as shown in Fig 4:

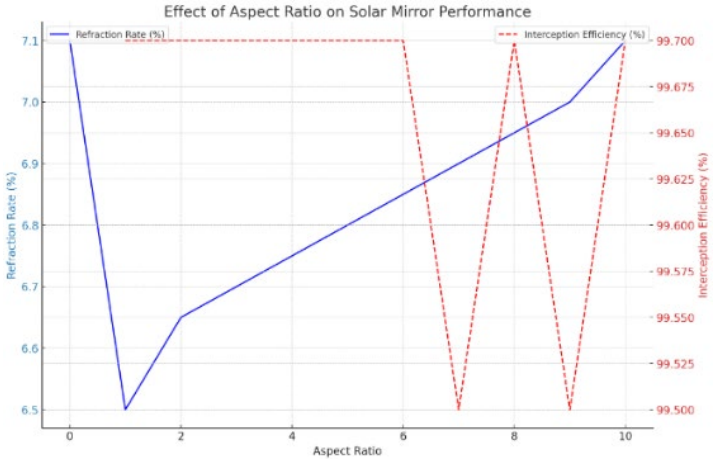

Figure 4: Variation of Truncation Efficiency and Shadow Rate with Aspect Ratio

Hrough analysis in this paper, the optimal aspect ratio can be obtained to optimize the performance of the heliostat field.

The aspect ratio has minimal significant impact on the annual average truncation efficiency of the heliostat (represented by the red dashed line). Within the aspect ratio range from 1 to 5, the truncation efficiency remains stable at 99.7%. However, within the range from 5 to 10, the truncation efficiency shows a sawtooth pattern of changes, but overall remains above 99.5%.

At the same time, the refraction rate (represented by the blue solid line) decreases first and then increases with the increase in the aspect ratio. When the aspect ratio is equal to 1, the refraction rate reaches its minimum value, about 6.5%.

Therefore, in the process of designing the structure of heliostats, more attention should be paid to the impact of the aspect ratio on optical efficiency. To maximize the efficiency of heliostats, those with an aspect ratio close to 1 should be used, as this not only minimizes the shadow rate but also maintains a high truncation efficiency.

3.2 Objective Function, Constraints, and Related Parameter Representation

In a single-stage reflective heliostat field, the absorption tower is usually located at the center of the site to maximize the thermal contribution of all heliostats. With the absorption tower as the point (0,0), a two-dimensional coordinate system can be established to describe the entire site.

ISSN 2616-5805 Vol. 5, Issue 1: 48-57, DOI: 10.25236/AJMS.2024.050108

(1)Objective Function

$$\text{MaximizeQ} = \frac{1}{\text{A}\times\text{N}\times 60}\sum_{\text{i}=1}^{12}\sum_{\text{j}=1}^{5}\text{P}_{\text{total}}(\text{i},\text{j}) \tag{27}$$

Where Q is the annual average output thermal power per unit mirror area; A is the area of a single heliostat, calculated as A = *mirror length* × *mirror width*; $N$is the number of heliostats; $P_{total}(i,j)$is the total thermal power of the heliostat field at the i month's j time point (9:00, 10:30, 12:00, 13:30, 15:00); i is the month, from 1 to 12; j is the time point of the month, from 1 to 5 (corresponding to 9:00, 10:30, 12:00, 13:30, 15:00).

(2)Parameters

Absorption tower height: 80m; Collector size: height 8m, diameter 7m; Heliostat size: mirror length and width between 2m to 8m; Heliostat installation height: between 2m to 6m.

3.3 Optimization Layout Based on Campo Method

$Campo$ is a circular heliostat field layout method proposed by $Collado$ et al.which can generate a flexible and regular radial staggered heliostat field. The Campo rule arranges the radially staggered heliostat field starting from the first row of the first layout area. The radiusR_1 of the first row is calculated based on the number of heliostats in the first row. Place the first heliostat at the due north of the first row, and the rest are evenly distributed circumferentially on the principle of avoiding mechanical collisions. If the heliostats are arranged in the densest way, the geometric relationship between the heliostats is as shown in Fig 5:

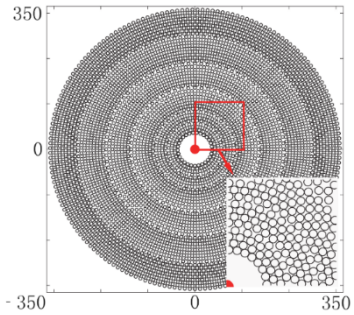

Figure 5: Geometrical Relationship Between Heliostats

In the $Campo$ layout method, heliostats are usually arranged starting from the absorption tower, on various concentric circles around the tower. The number of mirrors on each concentric circle and the distance between them can be determined according to specific optimization criteria .

In this paper, there are a total of 1745 heliostats in the entire field, so the number of heliostats in the initial field should be three times that of the target field (about 6000). In this case, the goal is to arrange about 6000 heliostats around the absorption tower using the $Campo$ layout method and then optimize further. Specific optimization requirements include:

No heliostats are installed within a 100m radius around the absorption tower, the size of each heliostat is between 2m and 8m, and the distance between the bases of adjacent heliostats should be more than 5m greater than the width of the mirror surface. All heliostats are installed at the same height, which is between 2m and 6m. In the same area, the number of heliostats per row is the same, with odd and even rows staggered, and the radial spacing between consecutive rows remains constant. The minimum increment $\triangle R_{min}$ between adjacent rows is calculated by$\triangle R_{min} = 0.866DM$, where DM s the diameter of the heliostat. The reflectivity of the mirror surface is 93%, and the shadow blockage efficiency is 99.97%. Finally, a layout scheme is found to achieve an average annual output of 60MW. The dense initial heliostat field generated based on the above parameters is shown in Fig 6 (heliostats are represented by circles due to the small size of the picture):

ISSN 2616-5805 Vol. 5, Issue 1: 48-57, DOI: 10.25236/AJMS.2024.050108

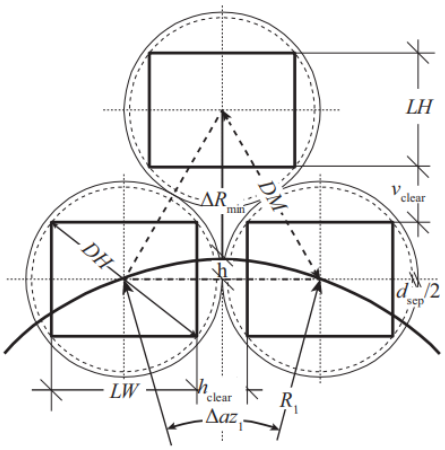

Figure 6: Dense Initial Mirror Field

Next, this paper uses the $SPA(Solar\ position\ algorithm)$ algorithm in $SolarPILOT$ simulate the position of the sun and calculate the annual average efficiency value (where, instantaneous values are simulated on the 21st of each month at 9:00, 10:30, 12:00, 13:30, 15:00 local time), and arrange according to efficiency. The arrangement results are shown in Fig 7:

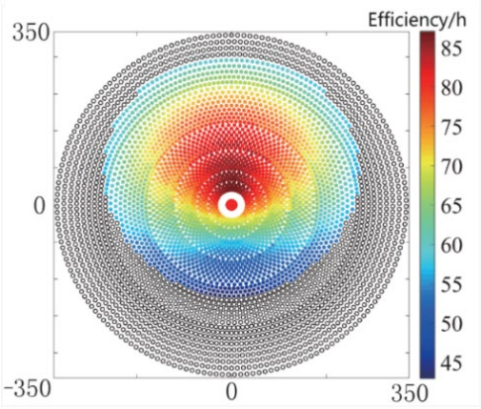

Figure 7: Annual Average Efficiency Values

From the optimization analysis, the final mirror field layout is approximately an ellipse skewed towards the north. In this configuration, the efficiency distribution is symmetrical left and right, but due to the mirror field being in the northern hemisphere, its northern efficiency is significantly better than the south. Compared to the previous target mirror field, the new layout scheme achieves a significant transient optical efficiency improvement of about 20%.

Therefore, once the required number of heliostats is calculated, the corresponding most efficient number of heliostats can be selected from these 6000 mirrors.

3.4 Using SQP Method to Solve for Optimized Mirror Field Layout

Based on the annual average output thermal power per unit mirror area fitted by $SolarPILOT$, this problem can be transformed into :

$$\text{required total mirror area}(\text{m}^2) = \frac{\text{P(MW)}}{\bar{\text{S}}(\text{kW/m}^2)} \times 100 \tag{28}$$

$$\text{P} = \text{target power(MW)}$$

$$\bar{\text{S}} = \text{average annual thermal power output per unit mirror area}(\text{kW/m}^2)$$

To achieve a rated power of 60MW, approximately 83333.33m^2 of total mirror area will be needed.

Using the SQP solver, the optimal mirror field coordinates are derived based on the complete mirror field, and the results are visualized. The visualization result is shown in Fig 8:

ISSN 2616-5805 Vol. 5, Issue 1: 48-57, DOI: 10.25236/AJMS.2024.050108

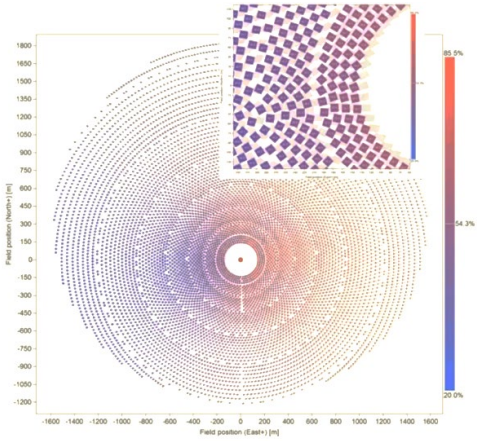

Figure 8: Visualization of the Optimal Mirror Field

4. Conclusion

The core of this study is to establish an optical efficiency and output thermal power model that combines the state of solar motion and relevant optical parameters. The main challenge faced in this paper is how to accurately calculate the shadow blockage efficiency, cosine efficiency, collector truncation efficiency, and handle a large amount of data. This paper derives an atmospheric transmittance model using geometric symmetry optimization methods and polynomial convolution methods. In addition, this paper also uses the law of reflection to vectorize light rays, thus building a cosine efficiency model with precision and robustness.

On the basis of the first step, this paper first determined the optimization conditions. By analyzing the relationship between truncation efficiency and shadow rate with the aspect ratio of the mirror surface, it was found that mirrors with an aspect ratio close to 1 have higher efficiency. Subsequently, algorithms were used to optimize the heliostat configuration and further reduce the constraints. Finally, the remaining constraints are listed, and the optimal solution is directly obtained using a solver.

In summary, this study not only proposes a new optimization method theoretically but also proves the effectiveness of this method in practice. The results of this study are of great significance for improving the efficiency and output performance of solar thermal power generation systems and provide a solid theoretical foundation and practical guidance for future research in this field.

References

[1] Gao Bo, Liu Jianxing, Sun Hao, Liu Erlin. Optimization Layout of Heliostat Field Based on Adaptive Gravitational Search Algorithm [J]. Journal of Solar Energy, 2022, 43: 119-124.

[2] Zhao Mingzhi, Sun Hao, Miao Yiming. Wind tunnel experimental study on the influence of sand accumulation on the output characteristics of PV modules [J]. Journal of Chinese Society of Power Engineering, 2019, 39(9): 765-769, 776.

[3] Shi Zhipeng, Gong Jun, Wang Weizhi, et al. Study on the Influence of Ash Accumulation on the Reflectivity of Tower Solar Heliostats [J]. Thermal Power Generation, 2019, 48(06): 134-137.

[4] Du Yuhang, Liu Xiangmin, Wang Xingping, et al. Influence analysis on different concentrating strategies of heliostats in a tower solar thermal power station [J]. Journal of Chinese Society of Power Engineering, 2020, 40(5): 426-432.

[5] Cheng Xiaolong, Yin Yanguo, Ma Shaobo. Research on the Optimization Design of Tower Power Station Heliostat Field Layout [J]. Energy and Environment, 2018(2): 64-66, 70.

[6] Huang Yafeng, Bi Dawei, Li Yuanhong. Analysis of family PV power cost based on LCOE principle [J]. Journal of Northeast Electric Power University, 2019, 39(3): 1-7.

[7] Wagner M J, Wendelin T. Solar PILOT: a power tower solar field layout and characterization tool [J]. Solar Energy,2018,171:185-196

[8] Li C, Zhai R R, Liu H T, et al. Optimization of aheliostat field layout using hybrid PSO-GA algorithm [J].Applied thermal engineering, 2018, 128(8):33-41.

[9] Cruz N C, Álvarez J D, Redondo J L, et al. A twolayered solution for automatic heliostat aiming [J]. Engineering Applications of Artificial Intelligence, 2018, 72: 253-266.

[10] Suhil Kiwan, Abdel Latif Khammash. Investigations into the spiral distribution of the heliostat field in solar central tower system [J]. Solar Energy, 2018,164.